LIMNOLOGY
and
OCEANOGRAPHY

ASLO

Limnol. Oceanogr. 00, 2017, 00–00

doi: 10.1002/lno.10587

The differential response of kelp to swell and infragravity wave motion

Julia C. Mullarney ,* **Conrad A. Pilditch**
Coastal Marine Group, Faculty of Science and Engineering, The University of Waikato, Hamilton, New Zealand

Abstract

We present field measurements of the movement of the giant kelp *Macrocystis pyrifera* under wave forcing. We resolve the depth and frequency-dependent responses along the stipe and find different and counterintuitive patterns of response at the infragravity and swell wave forcing frequencies. At swell frequencies, tilting of the stipe is largest toward the holdfast, whereas at infragravity frequencies, the stipe tilting is largest closer to the water surface. It is postulated that the stretching of blades and subsequent pull on the stipe is, in part, responsible for these patterns. This conclusion is supported by results of manipulative experiments, which show a more along-stipe uniform response after removal of blades from the kelp. The length of the kelp also exerts a strong control on the relative magnitudes of movements in the different frequency bands, with the swell band becoming more important relative to the infragravity band for shorter length kelp. These results indicate that kelp will differentially dissipate energy over both frequencies and varying depths within the water column. The variety of movement responses over differing wave forcing frequencies may also imply that there exist differing rates of breakage for kelp exposed to hydrodynamics stressors of multiple frequencies.

Macrophyte ecosystems offer many ecosystem services such as providing critical habitat for many species (Zedler et al. 2001; Greenberg et al. 2006), trapping contaminants and nutrients (Ward et al. 1984; Philips 1989; Gribsholt et al. 2007) and influencing coastal morphology (Kastler and Wiberg 1996; Bartholdy et al. 2004; Deegan et al. 2012).

The ability of vegetation to dissipate both tidal currents (e.g., Fonseca et al. 1982; Nepf 1999; Rosman et al. 2007) and wave energy has been widely noted (Knutson et al. 1982; Fonseca and Cahalan 1992; Möller et al. 1999). However, the extent of this dissipation depends strongly on the flexibility of the plant (Mullarney and Henderson 2010), which controls its ability to "go with the flow." Indeed, Riffe et al. (2011) found wind wave dissipation in salt marshes was substantially reduced (to 30% of that for equivalent rigid stems) by the tendency of the sedge *Schoenopletcus americanus* to bend with the waves. This ability to move with the surrounding water reduces the drag forces experienced by the plant and ultimately, rates of breakage (e.g., Koehl 1984; Denny and Gaylord 2002; Chapman et al. 2014).

For highly flexible species such as kelp, questions remain as to the precise nature of the balance between ability to move with the flow and the ability to damp wave energy (Mullarney and Henderson in press). Work conducted to examine the bulk dissipation of swell waves by large *Macrocystis* kelp beds in California found little dissipation (Elwany et al. 1995); whereas Rosman et al. (2013) used kelp mimics in a wave flume to conclude that wave orbital velocities within the canopy are reduced through conversion of the orbital wave energy into dissipative wake-scale eddies. At the scale of individual plants, previous observations and modelling have further indicated that forces experienced depend on position along the stipe. Additional inertial forces can be applied to the blade mass once fully extended, which can be characterized by a "jerk index," a parameter that is dependent on the wave forcing frequencies, and the mass and natural resonance frequencies of the kelp (Denny et al. 1998). Indeed, even flexible kelp species were found not to move with the surrounding water close to the sea bed (Stevens et al. 2001, 2002). This previous work measured accelerations at two locations on *Durvillea antarctica* blades, however, as this species inhabits the low intertidal zone and has a short stipe (<0.5 m long), the depth-dependence of movement along the stipe could not be captured. A more complete understanding of how plant and water motion differ along the stipe length for species growing vertically from the sea bed would allow for better prediction of how energy is dissipated throughout the entire water column.

*Correspondence: julia.mullarney@waikato.ac.nz

In a highly productive ecosystem with competition for space, the ability of kelp to "tune" their morphological structure and to engineer its surroundings can promote survival (e.g., Gaylord et al. 2003; Denny 2006; Demes et al. 2013). Variations in kelp morphology have been documented along flow gradients (e.g., Hurd et al. 1996) and alter in response to changes in flow regime (Koehl et al. 2008) indicating a response to mechanical cues. This response of kelp to mechanical cues encapsulates multiple feedback mechanisms and trade-offs. For example, a more upright posture, although resulting in more drag, may reduce self-shading (Koehl and Alberte 1988; Stewart 2006). Juvenile kelp must also reach a critical size before "going with the flow" can be considered advantageous (Denny et al. 1997). The rigidity and shape of kelp blades influence the velocity boundary layer at the blade surface, which controls nutrient uptake (Hurd et al. 1997; Hurd and Pilditch 2011; Rominger and Nepf 2014) and growth rates (Hepburn et al. 2007). Although previous studies have analyzed movement of isolated individual sections of kelp (e.g., Stevens et al. 2002 placed force transducers and accelerometers on *D. antarctica* blades), these studies did not consider the contribution of these elements (e.g., the blades) to the overall movement of the kelp.

In this paper, we present field observations of the motion of the giant kelp *Macrocystis pyrifera* under non-breaking swell and infragravity (periods of ~60 s) waves. The movement of an isolated individual was simultaneously captured at different heights along the length of the stipe using a series of accelerometers attached at fixed intervals. Using this approach, we resolved the differential frequency-dependent responses along the stipe, with lower parts of the kelp appearing to bend more strongly in response to the swell waves than the upper sections. Conversely, the sections of the stipe that sit higher in the water column, tilted further away from the vertical in response to forcing at the longer infragravity periods. Additionally, we undertook manipulative experiments removing different sections of the kelp to explore the relative contributions of morphological features to the large-scale movement of the kelp.

Field measurements

Field site

Observations were taken at the entrance to Otago Harbour in the South Island of New Zealand (45.775°S, 170.71°E). The field site encompassed a wave-exposed region open to Pacific swells and a more sheltered (harbor) region on either side of a breakwater (Fig. 1). A *M. pyrifera* kelp forest lines both sides of the breakwater in water depths of around 3–5 m.

Data acquisition and processing

Experiments were undertaken over 3 d during the early austral summer (December 2013) (Table 1). Kelp specimens were collected by divers from the sheltered side of the breakwater (as diver observations indicated that kelp on this side tended to be taller) and bought on shore. HOBO Pendant G Accelerometers (with a resolution of 0.025 g and accuracy varying between ± 0.075 g and ± 0.105 g, depending on temperature) were attached at fixed intervals up the stipe bundle (Table 1; Fig. 2a). The sensors measured accelerations in three axes relative to the sensor (here, denoted g_x, g_y, and g_z) at 4 Hz (Fig. 3). Here, for small tilts or displacements, z depicts accelerations in the near-vertical direction whereas and x and y show near horizontal motions. The instrumented kelp consisted of several entwined stipes originating from a single holdfast. For the purposes of the work presented here, the movement of the whole stipe bundle was considered as that of a single entity (hereafter referred to as stipe). Measurements were made of the stipe count, individual stipe thicknesses, and the thickness of the whole "stipe bundle" along the length of the kelp. The holdfast was firmly tied to a weight and the kelp returned to the water within an hour of being collected and during this time it did not dry out. Kelp were placed on either side of the breakwater on different days to allow

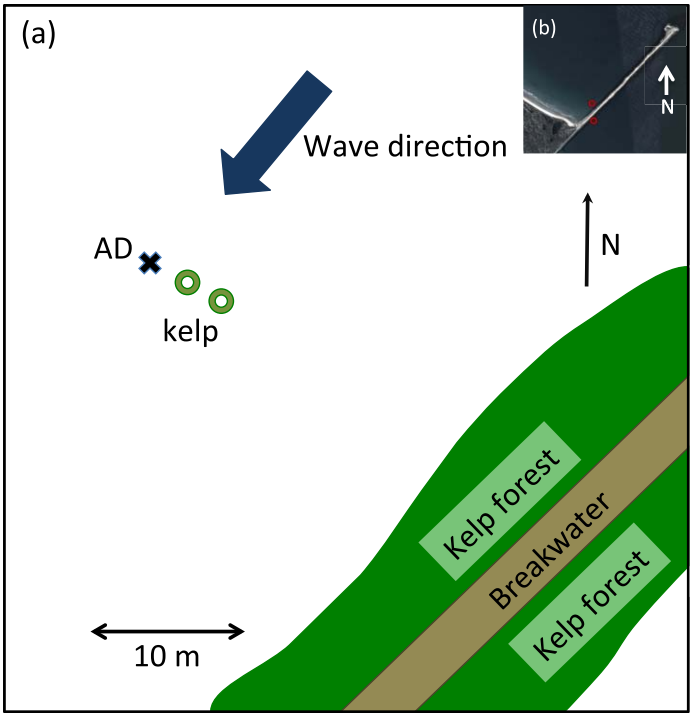

Fig. 1. (**a**) Schematic showing example experimental array. Pictured is the deployment from day 3 (*see* Table 1) on the northern side of the breakwater. AD indicates the Nortek Aquadopp ADCP. (**b**) The inset shows deployment locations from all 3 d (red circles) with instruments and kelp placed south of the breakwater on days 1 and 2, and north of the breakwater on day 3. In (**b**) the scale is given by the length of the breakwater, which is approximately 950 m.

Table 1. Summary of experiments performed.

Day	Number of kelp instrumented	Maximum stipe length (m)	Number of accelerometers	Accelerometer spacing (m)	Significant wave height (m)	Mean water depth (m)	Manipulation
1	1	4.7	10	0.5 (#'s 1–9) 0.2 (#'s 9–10)	0.25	5.6	Blade removal
2	1	3.6	9	0.4	0.32	5.9	Stipe shortening
3	2	2.2	5	0.4	0.37	3.4	No change
		2.0	5	0.4			Stipe shortening

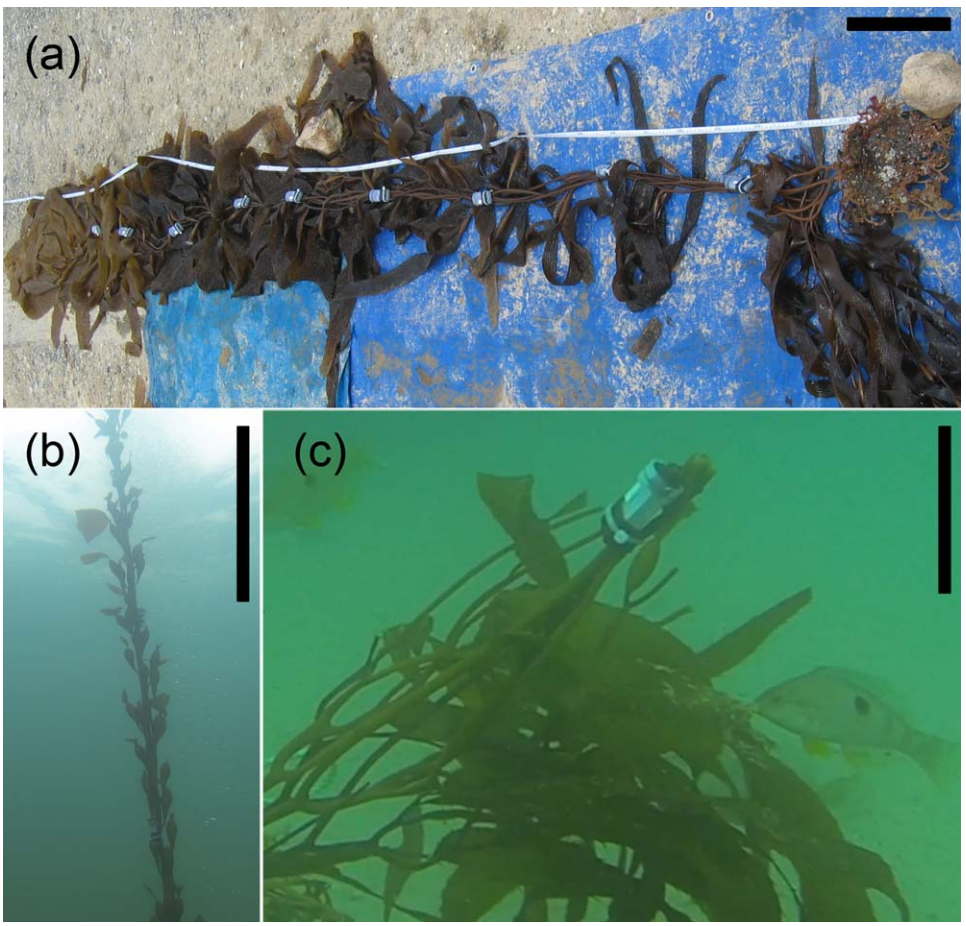

Fig. 2. (**a**) Instrumented kelp from day 2 with accelerometers attached at 0.4 m intervals. The stipe bundle was 3.6 m long and consisted of six fronds close to the holdfast reducing to a single frond at the top of the kelp. This sample exhibited the typical observed (from this field site) structure of small blades near the holdfast, a barer middle section and more and longer blades toward the top of the kelp. Photographs showing manipulations performed on kelp. (**b**) Blade removal (day 1). (**c**) Shortening – in this case the accelerometer is 0.4 m above the holdfast (just outside of the bottom left of the image) and the remaining kelp above has been removed (day 2). The black scale bar corresponds approximately (as effects of parallax are not considered) to lengths of 0.4 m (panels **a** and **b**) and 0.1 m (panel **c**).

measurements under a slightly wider range of wave conditions. Individual kelp were placed a small distance away from the forest (10–20 m) to remove any potential sheltering effects from other kelp (Fig. 1). The accelerometers were synchronized in time by pulling the in situ kelp rapidly downwards at a known time.

Pressure and water velocities were measured by a Nortek 2 MHz Aquadopp Acoustic Doppler Current Profiler (ADCP),

deployed a few metres away from the kelp (Fig. 1) at depths of ca. 5.6 m, 5.9 m, and 3.4 m on days 1, 2, and 3, respectively. The instrument and kelp were oriented to form a line approximately perpendicular to the anticipated wave propagation. The ADCP operated in "pulse to pulse coherent" mode to resolve pressures and velocities close to the seafloor at high temporal and spatial resolution (4 Hz temporal with a vertical resolution of 25 mm over a total profile lengths of 0.55 m, days 2 and 3).

After the movement of the unaltered kelp was measured for at least 45 min, additional manipulative experiments were undertaken. On day 1, all blades were removed from the fronds leaving just the stipe bundle and pneumatocysts (Fig. 2b). On days 2 and 3, kelp were cut to successively shorter lengths by removing the top 0.4 m of the stipe bundle every 5–10 min (Fig. 2c). Movement responses were characterized by the sum of the spectra of the tilts from all three axes ($S_{xx} + S_{yy} + S_{zz}$). The spectra were calculated using Hanning-windowed data segments with 70% overlap and the resulting frequency resolution was $\Delta f = 0.0039$ Hz. Additionally, divers undertook visual observations and video recordings throughout each experiment.

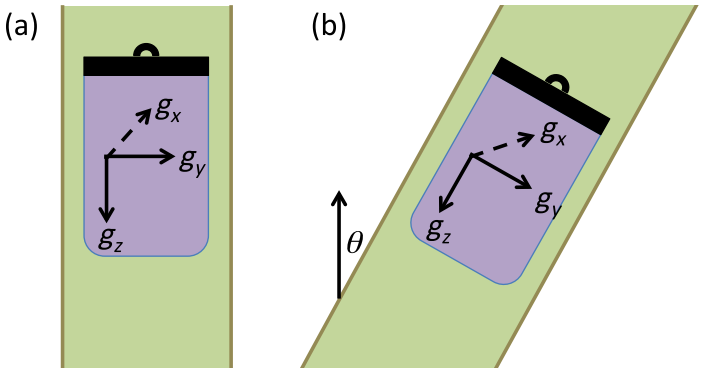

Fig. 3. Axes orientations on (**a**) vertical kelp and (**b**) tilted kelp. Note the *z* coordinate is near-vertical positive downwards and the *x* and *y* coordinates are near-horizontal for small tilts or displacements.

Results

Environmental forcing conditions

Wave conditions were similar during all 3 d of the experiment. Linear wave theory was used to correct for the depth-attenuation of pressure signals and to transform from measured values at the sea floor to surface values (with a cut off

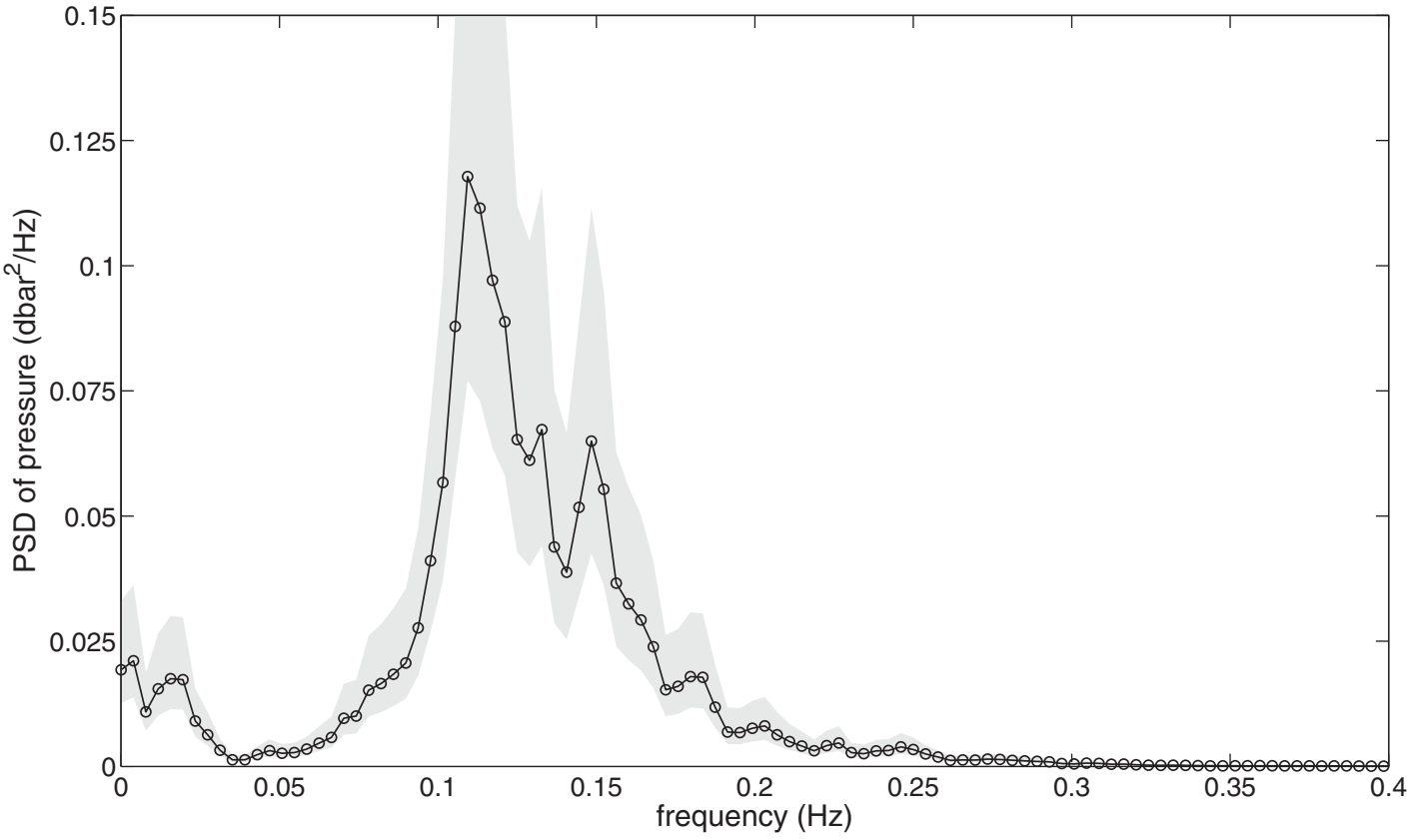

Fig. 4. Day 3 representative power spectral density of pressure data from the high resolution ADCP corresponding to the period during which kelp accelerometer data was collected. The main peak corresponds to the swell period (~ 9 s) and the secondary low-frequency peak corresponds to the infra gravity wave period (~ 64 s). The gray shading indicates the 95% confidence intervals.

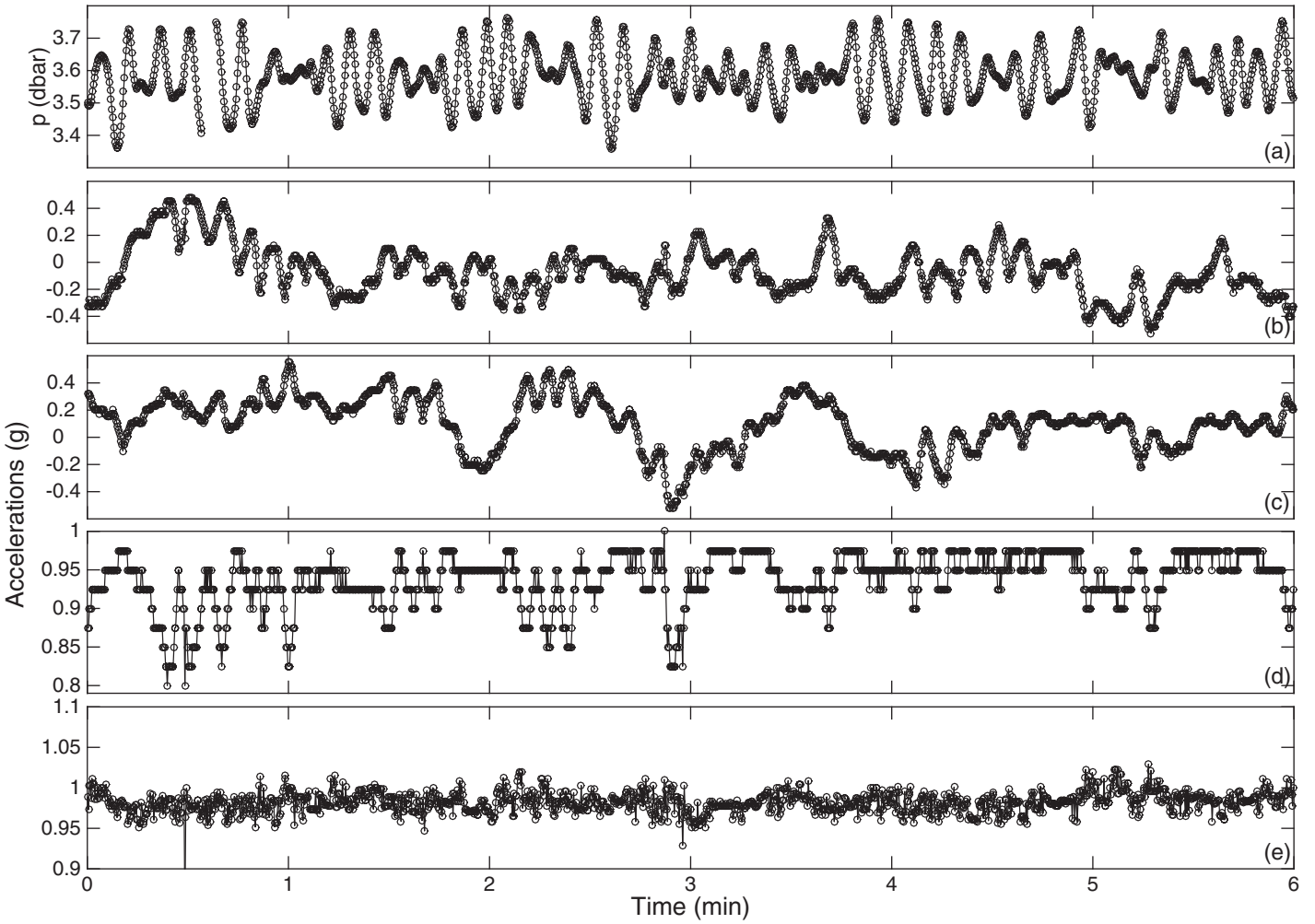

Fig. 5. Day 3 example time series of pressure from the ADCP (**a**) and associated stipe accelerations from the accelerometer ((**b**) *x*, (**c**) *y*, and (**d**) *z*, axes) close to the mid-height of the un-manipulated kelp (1.2 m above the holdfast). Panel (**e**) shows the acceleration magnitude $\sqrt{g_x^2+g_y^2+g_z^2}$.

frequency of 0.3 Hz). Significant wave heights were estimated as four times the standard deviation of the detrended sea-surface elevations as 0.25 m, 0.32 m, and 0.37 m over the 3 d. Spectral analysis of pressure measurements indicated that the dominant forcing frequency was the swell frequency ($f \sim 0.11$ Hz, $T \sim 9$ s), however there was also energy at the lower infragravity wave frequencies ($f \sim 0.016$ Hz, $T \sim 64$ s) (Fig. 4). Water depths were sufficient to ensure there was essentially no surface canopy for the instrumented kelp during measurement periods, with the exception of day 1 measurements when a few blades and the scimitar blade (the apical blade at the top of the kelp) occasionally touched the surface.

Resolving kelp movement from accelerometers

Example time series of raw accelerations from the mid-height of a single kelp (1.2 m above holdfast, prior to any manipulation) are shown in Fig. 5 along with the corresponding ADCP pressure time series. At this time, diver observations confirmed that the accelerometers were sitting approximately upright on the full-length kelp with the exception of the sensor placed closest to the top of the kelp (which was tilted closer to 30°, not shown). Both the swell and infragravity wave signals can be discerned in the response. In particular, the *y*-axis measurements (Fig. 5c) show smaller oscillations at the swell frequency (amplitudes of ~ 0.15 g with periods around 9 s) superimposed on large, longer period oscillations (amplitudes of ~ 0.5 g with periods of around 1 min).

The sensors cannot distinguish between acceleration changes due to tilt and those due to translation (the problem is mathematically unconstrained with six degrees of freedom and only three variables measured), noting that the sensors will record the gravitational acceleration of 1 g when at rest. Similarly, a stationary but tilted sensor will also record acceleration components relative to the reference frame of the sensor and hence can also act as a tilt sensor

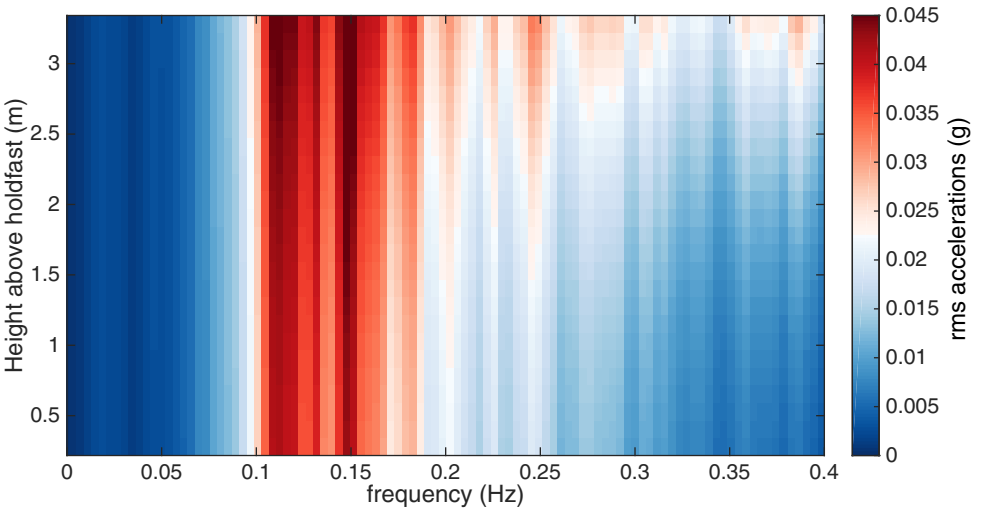

Fig. 6. Day 3 root-mean-squared horizontal accelerations of water particles typical of the experimental period estimated from the pressure spectra using linear wave theory (cut-off frequency 0.4 Hz).

(Marchant et al. 2014). In this experiment, the magnitude of accelerations $\sqrt{g_x^2+g_y^2+g_z^2}$ (Fig. 5e) remained close to 1 g throughout the deployment (typically varying between 0.95 g and 1.05 g), thus implying that rotation or tilt of the sensor was predominantly responsible for the fluctuations in the individual components of acceleration. We note that tilts of approximately 50° and 15° from the vertical would be required to give the acceleration changes observed in the infragravity and swell bands, respectively and these values are indeed consistent with diver observations.

Additionally, we assume that the horizontal accelerations of the water particles place an upper bound on the kelp acceleration that could arise from translatory motion. This assumption is likely valid, for example in the case of the day 3 un-manipulated kelp which extended nearly to the surface and was forced by relatively small unbroken waves. However, we note that this assumption would not be universally valid. Under larger waves, kelp which has reached its furthest excursion may experience substantial inertial forces as it decelerates and jerks backwards (Denny et al. 2006, 1998). The root-mean-squared horizontal accelerations (in g) of the water particles were estimated from the pressure spectra using linear wave theory as $\sqrt{(gk)^2 S_{\mathrm{pp}}/g}$ where k is the radian wavenumber relation at each radian frequency ($\omega = 2\pi f$) obtained by inverting the surface gravity wave dispersion relation and S_{pp} is the auto-spectra of pressure (Simpson 1969). For all depths and frequencies, these accelerations ($\sim$ 0.05 g) were an order of magnitude smaller than those observed from the accelerometers ($\sim$ 0.5 g, Fig. 6). Hence, we conclude that the dominant signal in the data is owing to the tilt of the accelerometers rather than translatory motion. Consequently, hereafter the response of the kelp will be characterized by the tilt angles, using the sum of the spectra of the tilts from all three axes, here denoted $S_{xx} + S_{yy} + S_{zz}$.

Response of un-manipulated kelp

The spectra of tilts revealed the existence of differential responses over the kelp length (Fig. 7). A somewhat counter-intuitive result was observed: the lower sensors appeared to respond more strongly (i.e., the kelp tilted further from the vertical) to the energy in the swell band (Fig. 7b) than the sensors attached high up the kelp and close to the surface, whereas the opposite effect was observed in the infragravity energy band (Fig. 7a), although differences (i.e., tilts) between sensors were subtle over most of the stipe length. This pattern was most clearly discerned on day 3 which experienced the largest wave forcing, however it was observed in all measurements of un-manipulated kelp (after excluding the accelerometer closest to the top of the kelp which was often tilted past 90°). This differential response with depth and frequency has consequences for the shape of the kelp stipe. Given the measurements at both frequencies are dominated by tilt (Fig. 6), then this pattern of response implies that the infragravity energy tends to bend the kelp in a concave downward shape, whereas the swell frequencies promote a convex downward curve (Fig. 7 - insets).

Response of manipulated kelp

During the manipulative experiment on day 1 (Fig. 2b), the intact kelp exhibited movement consistent with that shown in Fig. 7; that is, the strongest response at swell frequencies occurred closer to the holdfast (with the exception of the top sensor at 4.5 m, Fig. 8a). However, after the removal of the blades leaving only the stipe and pneumatocysts, the movement and bending responses were more uniform with depth, as indicated by the spectral curves from

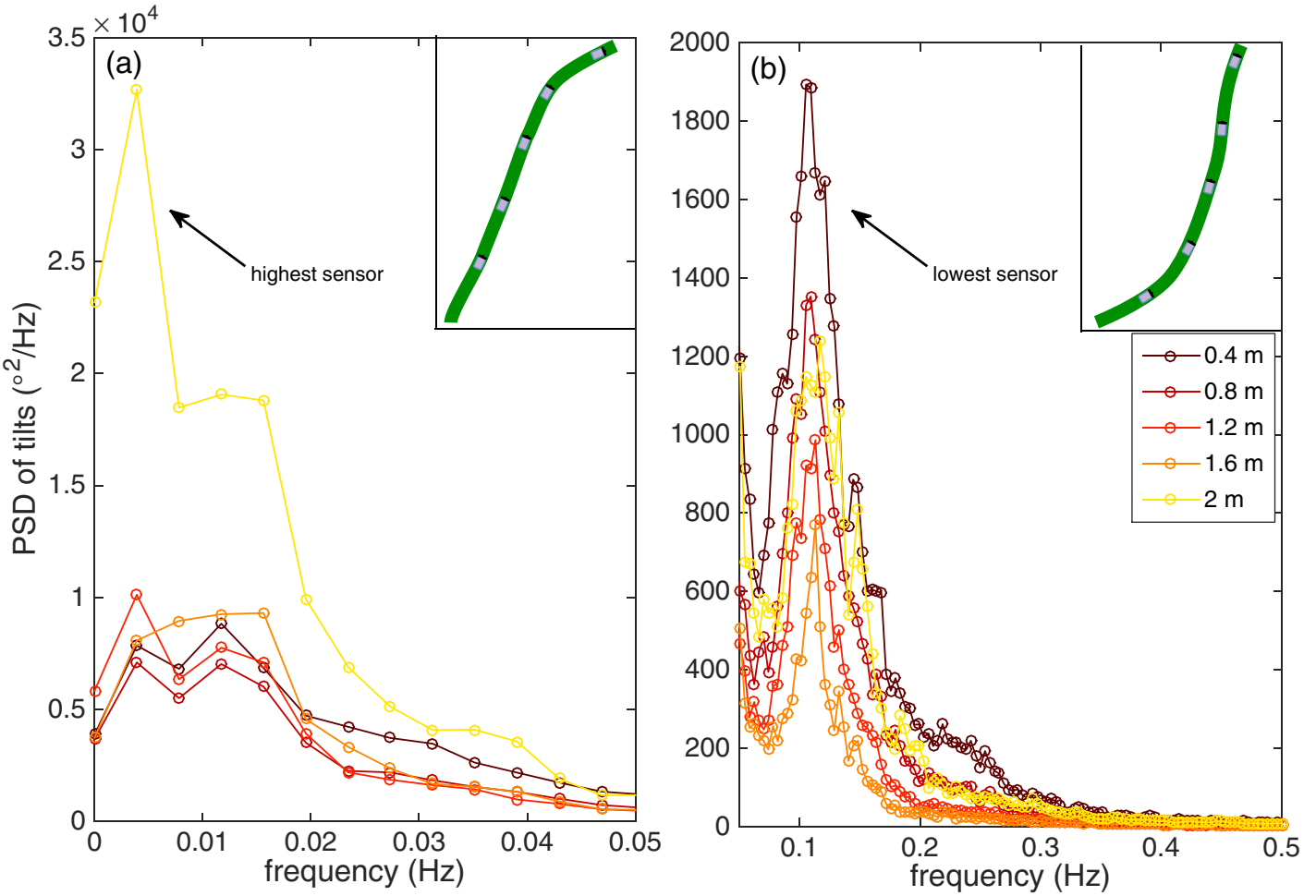

Fig. 7. Day 3 power spectral densities of tilts (sum of all three axes, $S_{xx}+S_{yy}+S_{zz}$) from sensors at different heights above the holdfast (indicated by colors) of the un-manipulated kelp. Each data record was 48 min long and the spectra have 29 degrees of freedom. Responses at (**a**) infragravity (0–0.0625 Hz), and (**b**) swell (0.0625–0.172 Hz) frequencies. Insets show a schematic of kelp shape implied from the spectra of tilts. Note the change in *y*-axis scale between (**a**) and (**b**) and that the displacements shown in the insets are not to scale – the tilting associated with the infragravity frequencies is approximately 5–10 times larger than that associated with swell frequencies.

different heights collapsing onto each other (Fig. 8b). However, the magnitude of the accelerations did not change significantly in either frequency band.

The shortening of the kelp also had a substantial effect on both the pattern and magnitude of movement. As the top sections of the kelp were successively removed, the movement of the lower sections is less constrained and we see the response of larger tilts of the remaining kelp in the swell band (Fig. 9). In particular, for very short kelp (lengths of around 0.4–0.7 m; Fig. 2c), the accelerometers recorded large "accelerations." In these cases, visual observations noted substantial "jerking" of the kelp and hence contributions to accelerations are likely composed of both tilting and also translatory movement (Fig. 9d–f). The deformed shape of the stipe cannot be explicitly determined from the data, as the stipe bundle rotates and hence the sensor orientation (heading) is unknown. However, it possible to form an estimate of the general shape of the stipe by considering only the *z*-direction tilts (Fig. 3). Estimates of the shape of the deformed stipe are shown for the experiment on day 3 in Fig. 10. Each shape is a snapshot from a single point in time (we used the third largest peak in *z*-tilt from the uppermost sensor as a representative example of a time with large displacements). The overall shape is shown in panel (a). The time series of tilt are low and high pass filtered with a frequency cut of 0.033 Hz (i.e., a cut-off period of 30 s) to estimate tilting due to infragravity (Fig. 10b) and swell motions (Fig. 10c), respectively. The overall shape is dominated by the infragravity motions, however, the relative importance of the swell motions increases toward the holdfast.

The results for the experiments examining the effects of shortening the kelp (days 2 and 3) are summarized in Fig.

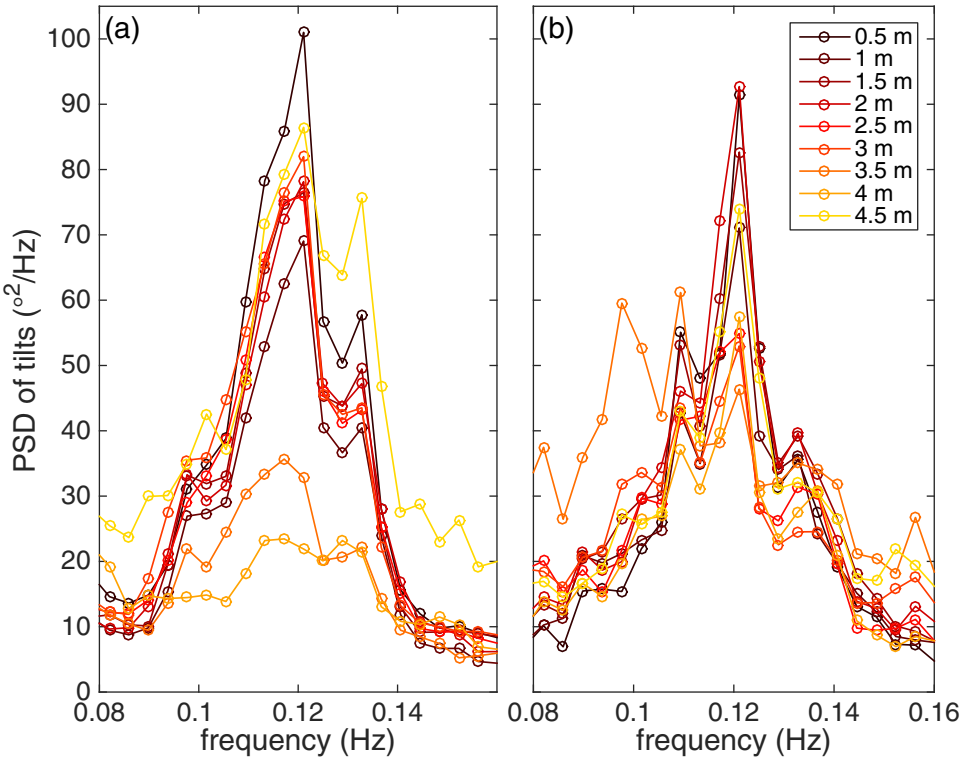

Fig. 8. Day 1 power spectral densities ($S_{xx}+S_{yy}+S_{zz}$) of tilts in the swell (0.0625–0.172 Hz) frequency band before (**a**) and after (**b**) blade removal (*see* Fig. 2b). Colors indicate sensor height above the holdfast. The data from the full-length kelp was recorded for 58 min (spectra have 36 degrees of freedom) and post-manipulation accelerations were recorded for 17 min (10 degrees of freedom).

11. Panel (a) shows the rms tilt angles $\sqrt{\int (S_{xx}+S_{yy}+S_{zz})\ \mathrm{df}}$ across the infragravity frequency band. For almost all kelp the top experiences larger tilts than the bottom (shown by positive gradients of linear fits). The opposite trend (larger tilting near the holdfast, negative gradients for linear fits) is observed for the motions in the swell frequency band. A single exception to this pattern was observed in the full-length kelp on day 3 (light yellow triangle) for the uppermost sensor which was strongly tilted. As the kelp is successively shortened (decreasing l/h, where l is kelp length and h is water depth), movement in both frequency bands increases. For the cases with the shortest kelp, only one accelerometer remained on the kelp so no fit lines are shown, but the single values indicate much stronger tilts and movement (dark blue symbols). The patterns between different heights of kelp remained the same on day 2 and 3, the difference being that on day 3 with stronger forcing (a combination of larger wave heights and lower water depths, triangles on Fig. 11), the overall magnitude of responses were stronger. The data indicate the presence of a "critical length" below which movement of the kelp changes substantially. For taller kelp ($l/h > 0.5$, yellow and green points, Fig. 11a,b) responses are similar, however once the kelp has been cut down to shorter than this critical length, the accelerations and tilting increase substantially (blue points). This change in movement is also accompanied by a dramatic change in the relative magnitudes of the infragravity to swell motions indicated by the maximum value of the tilt spectra from all accelerometers in their respective frequency bands (Fig. 11c). Although there is some scatter, for higher values of l/h ($\gtrsim 0.5$) the energy in the infragravity frequencies is around an order of magnitude larger than in the swell bands, however, for short kelp ($l/h \lesssim 0.5$), the energy in the swell band is of the same order of magnitude (and in two examples is greater than) that in the infragravity band.

Discussion

The results shown above demonstrate that kelp moves differently in response to multiple forcing frequencies. We suggest that this frequency-dependent response is in part owing to drag from the blades preventing motion at the swell frequencies. Diver and video observations show the long blades toward the top of the kelp oscillating back and forth and stretching out at the lower infragravity frequencies but not the swell frequencies (Fig. 12). These observations are consistent with the length of these top blades ($\sim$ 1 m to 1.5 m) being longer than the horizontal orbit of water particles at

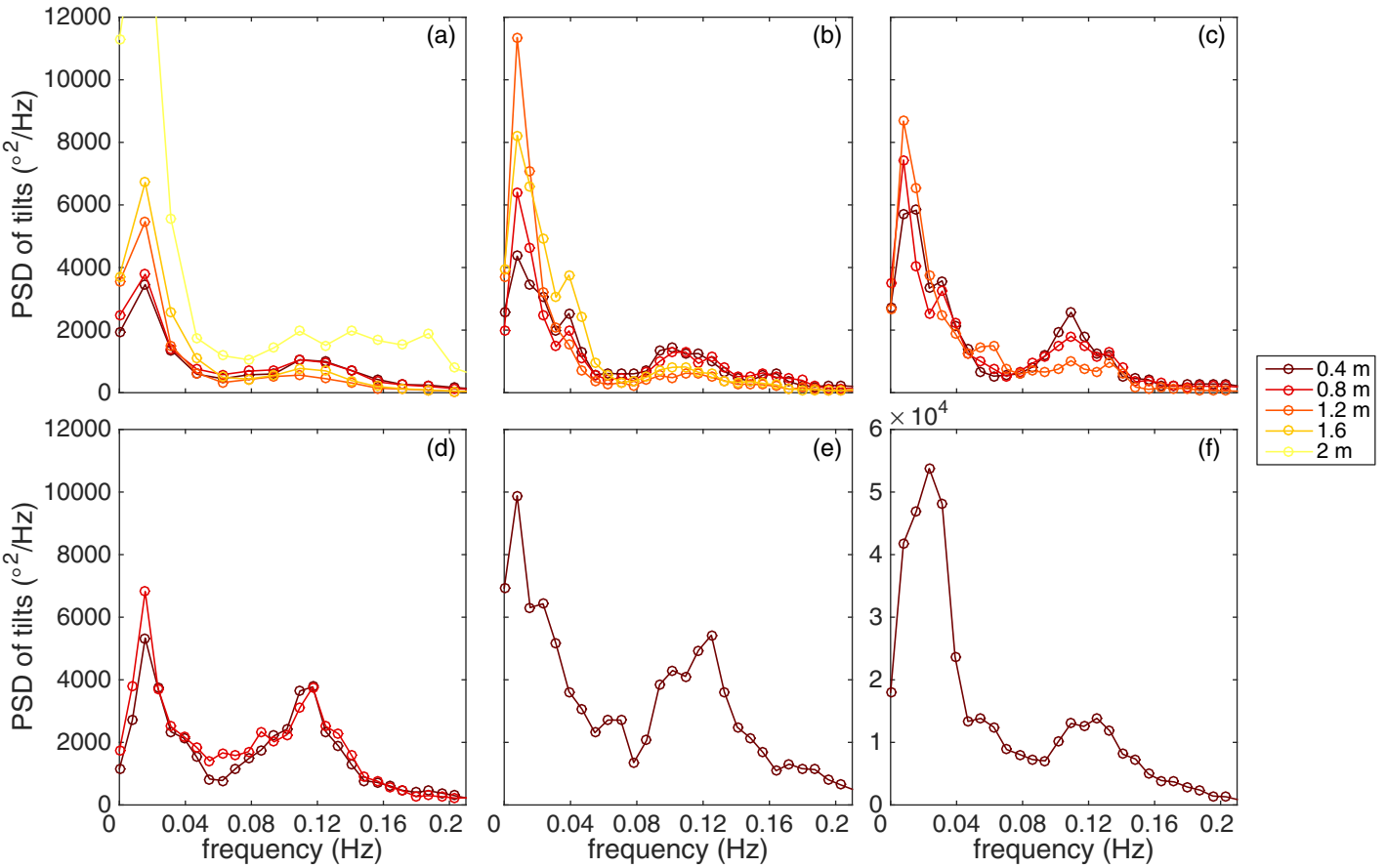

Fig. 9. Day 3 power spectral densities (PSD) of tilts (sum of all three axes $S_{xx}+S_{yy}+S_{zz}$) from sensors at different heights above the holdfast (indicated by colors) before (**a**) and after shortening of kelp from 2 m to: 1.95 m (**b**), 1.55 m (**c**), 1.15 m (**d**), 0.75 m (**e**), and 0.45 m (**f**). Note the change in scales on the vertical-axes in (**f**). In the response of the full length kelp (**a**) the PSD for the top sensor (2 m) reached a maximum value of ∼16,800. Each panel represents between 5.5 min and 10 min of data and the spectra have between 9 and 14 degrees of freedom.

the swell frequencies (∼ 0.3 m) but shorter than the orbital excursions of water particles at the infragravity frequencies (∼ 6 m). Hence, the blades closer to the surface do not exert any pull on the central stipe bundle at the swell frequencies, but the same blades are able to exert pull on the stipe at the infragravity frequencies. Closer to the holdfast, the blades are specialized sporophylls, which typically are much shorter and this short length allows them to be affected by the swell period motions (Fig. 12b). Diver observations noted vigorous jerking movements of the shortened kelp, (which may also possibly enhance spore release). This conclusion that drag from the blades plays an critical role is not new (e.g., Koehl 1984; Denny et al. 1997; Gaylord et al. 2008); however, the counter-intuitive pattern of movement found here highlights the complex nature of the balance between physical stressors and kelp movement.

The methods used in this experiment and resolution of the accelerometers precluded direct measurements of stipe displacements; however, future work will explore the possibility of using a six-axis accelerometer unit (including pitch, roll, and heading measurements) which should allow for separation between the accelerations resulting from tilt and from translation. We note that the actual kelp displacement is a superposition of the two (and other) modes and hence the response at individual frequencies cannot be discerned visually by divers.

Although we did not make detailed measurement of the movement of the blades themselves, the inference that the blades at the surface (which constitutes the majority of the biomass at least for the present field site) did not respond at the swell frequency has some interesting potential implications. If the blades are not moving with the swell frequencies, then there must consequently be a large relative velocity between the water and the blade surface. It is this relative velocity which aids in breaking down the diffusional boundary layers that limit the transport of dissolved solutes to and from the blade surface (Hurd and Pilditch 2011). To our knowledge, to date there have been no direct measurements of boundary layer thickness under orbital motion, but our results raise the intruiging possibility that the movement

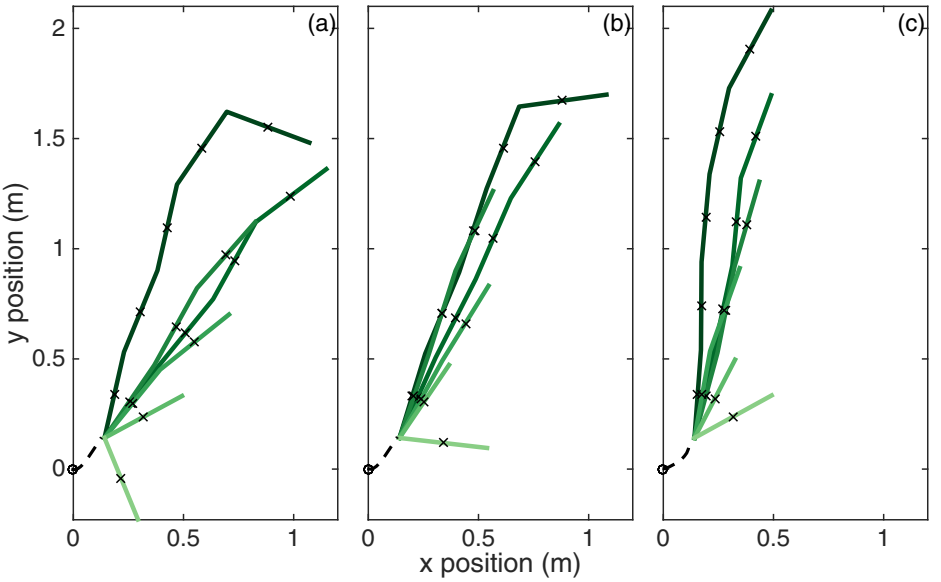

Fig. 10. Day 3 - approximate shape of deformed stipe estimated from the *z*-tilt. (**a**) All frequencies, (**b**) infragravity (low-pass filtered), and (**c**) swell (high-pass filtered) motions only. Colors show different kelp lengths: before shortening (dark green) and after shortening (lighter greens), corresponding to panels (**b**–**f**) from Fig. 9. Dashed line shows estimate for lower section of kelp joining first instrument to holdfast. Black crosses show locations of accelerometers.

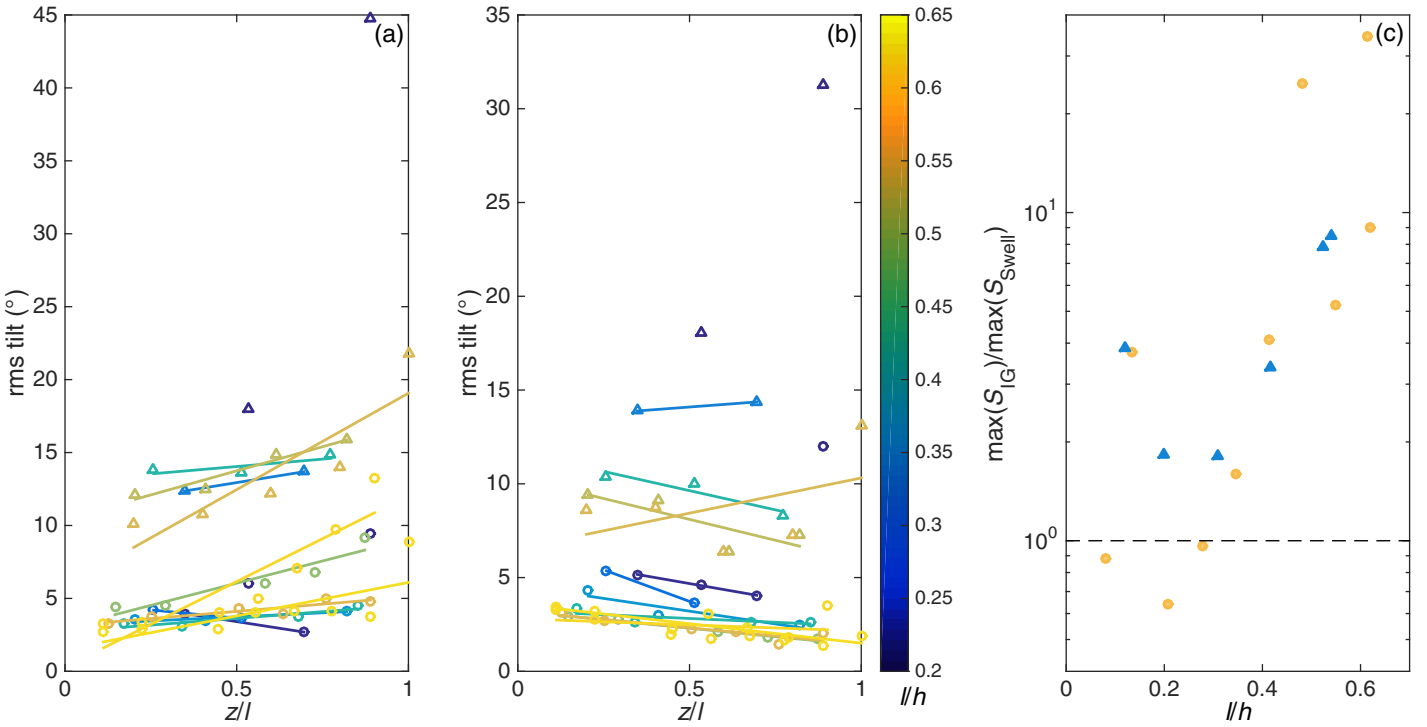

Fig. 11. Root-mean-squared (rms) tilts as a function of normalized position along the stipe (z/l where 0 is the holdfast and 1 is the top of the kelp) in the (**a**) infragravity (0–0.0625 Hz) and (**b**) swell (0.0625–0.172 Hz) frequency bands from the two experiments in which the kelp was successively shortened (days 2 and 3). Lines in (**a**) and (**b**) indicate a linear fit to the data for each stipe length and colors indicate the non-dimensional kelp length over water depth (l/h). (**c**) Ratios of the maximum value of the power spectral density of tilts ($S_{xx}+S_{yy}+S_{zz}$) in the infragravity (IG) frequency band to that in the swell frequency band as a function of non-dimensional kelp length. The dotted line indicates a ratio of 1. In all three panels circles and triangles show results from day 2 and day 3, respectively.

Fig. 12. Schematic showing how blade behavior varies along the stipe in response to (**a**) infragravity (upper near-surface blades) and (**b**) swell frequencies (lower near-holdfast blades). Figure adapted from Stephens and Hepburn (2016).

response observed here may promote thinner blade boundary layers, thus increasing uptake of nutrients and enhancing growth (*see* Hurd 2000 for a review of boundary layer dynamics).

A recent model developed by Luhar and Nepf (2016) describes the motion of flexible aquatic vegetation under wave-forced flows. The model is based on the Morison force formulation (Denny et al. 1998) and balances the deforming forces of drag with the restoring forces of buoyancy and stiffness. Numerical solutions of the analytical model were compared to results from laboratory experiments with seagrass mimics. Two limiting modes of behavior were found. For large horizontal wave excursions, seagrass deformations resembled those under unidirectional flow (Luhar and Nepf 2011); whereas for small wave excursions, the deflection behavior matches that described by Mullarney and Henderson (2010), in which forcing with longer (shorter) wave periods effectively means vegetation acts as stiffer (more flexible) vegetation. Although the Luhar and Nepf (2016) model represents a simplified case of the present field measurements by using a single "seagrass" blade (equivalent to a single stipe with no blades) with constant elasticity along its length, some aspects of their solutions qualitatively resemble the behaviors described here. Greater displacements and tilting were found for shorter vegetation as shown in Fig. 10. The infragravity-forced motion of smaller tilts closer to the sea bed and larger tilting of the stipe close to the surface is consistent with shapes found in the "stiff" vegetation case of Luhar and Nepf (2016). Conversely, the pattern of tilts under swell wave forcing resembles the patterns found for their solutions with more flexible vegetation—larger tilts at both the bottom and top of the stipe, with smaller tilting at mid-height.

The ability to attenuate wave and current energy depends on the drag at each height, a function of the difference between the water and plant motion. Thus, the frequency-

dependent responses shown here imply that kelp may differentially dissipate wave energy at different frequencies—a tendency that has been noted for other saltmarsh species (e.g., Bradley and Houser 2009; Mullarney and Henderson 2010) and for longer period frequencies in kelp (Jackson and Winant 1983 observed that semi-diurnal (tidal) frequencies were preferentially passed through a forest of *M. pyrifera*). The results additionally suggest that energy is differentially dissipated over depth in the water column. Such a frequency-dependent result may imply that even subtle shifts in forcing frequencies could induce damage to plants of particular heights (i.e., an increase in infragravity energy will affect taller plants more strongly than shorter ones), and hence change the morphological characteristics of whole communities.

Our work demonstrated that shortening kelp led to greater tilts and accelerations of the individual plants at the swell frequencies; in particular for very short kelp, the stipe appears to experience substantial jerking. This dependence on length may be a contributing factor toward field observations which have shown that juvenile *Macrocystis* plants are susceptible to thinning during autumn and winter storms (Graham et al. 1997; Reed et al. 2008). However, further experiments would be required to confirm a relationship between mortality and age/length and this work would need to include consideration of plant functional traits including the strength of the stipe (Thomsen et al. 2004).

The results presented here focus on an isolated kelp under a relatively limited set of field conditions with shallow water (depths < 6 m), small swell waves (maximum wave heights of around 0.5 m) (Fig. 4). However, *M. pyrifera* is often found in deeper water 7–20 m and exposed to much larger waves, such as on the West coast of the U.S.A. (North 1971). Under these conditions, for fully-submerged kelp, it is likely that the movement would also be a combination of the two modes of behavior described here depending on the values of parameters of the ratios of blade lengths to wave excursion and stipe lengths to wave excursion. However, *M. pyrifera* is often accompanied by substantial surface canopies (e.g., Reed and Foster 1984) with kelp lengths exceeding water depths so the tops of fronds lie horizontally on the water surface. In these cases, we anticipate the movement of the kelp may well be significantly altered from the patterns described here, with differences accentuated depending on the amount of surface canopy. Consequently, as noted by Gaylord et al. (2008), the stresses and breakage rates could be very different. Future work will explore changes in movement owing to surface canopies. Also, in the present work, a kelp was deliberately placed away from the forest in order to allow for examination of the movement of a single kelp in isolation. However, movement may be altered by interaction, and in particular entanglement, with other stipes of surrounding kelp. Koehl and Wainwright (1977) found the majority of breakage of intact stipes (i.e., not grazed) occurred following entanglement with other stipes.

We have measured the variable response of an isolated kelp to wave forcing with particular emphasis on resolving frequency-dependent differential responses along the stipe length. The kelp responds in a counter-intuitive manner to the swell frequencies with larger bending toward the bottom of the stipe. Conversely the top of the stipe appears to respond more to infragravity forcing than the lower sections. It is suggested that drag from kelp blades prevents movement of the higher sections of the kelp at swell frequencies, however the blades are shorter than water movements (and thus can be stretched out) at the infragravity frequencies.

References

Bartholdy, J., C. Christiansen, and H. Kunzendorf. 2004. Long term variations in backbarrier salt marsh deposition on the Skallingen peninsula - The Danish Wadden Sea. Mar. Geol. **203**: 1–21. doi:10.1016/S0025-3227(03)00337-2

Bradley, K., and C. Houser. 2009. Relative velocity of seagrass blades: Implications for wave attenuation in low-energy environments. J. Geophys. Res. **114**. doi:10.1029/2007JF000951

Chapman, J. A., S. Gulliver, and B. N. Wilson. 2014. Flume instrumentation for measurement of drag on flexible elements under waves. Exp. Fluids **55**: 1715. doi:10.1007/s00348-014-1715-7

Deegan, L. A., S. Johnson, R. S. Warren, B. J. Peterson, J. W. Fleeger, S. Fagherazzi, and W. M. Wollheim. 2012. Coastal eutrophication as a driver of salt marsh loss. Nature **490**: 388–394. doi:10.1038/nature11533

Demes, K. W., N. Pruitt, C. D. G. Harley, and E. Carrington. 2013. Survival of the weakest: Increased frond mechanical strength in a wave-swept kelp inhibits self-pruning and increases whole-plant mortality. Funct. Ecol. **27**: 439–445. doi:10.1111/1365-2435.12067

Denny, M. W. 2006. Ocean waves, nearshore ecology, and natural selection. Aquat. Ecol. **40**: 439–461. doi:10.1007/s10452-004-5409-8

Denny, M. W., P. Gaylord, and E. A. Cowen. 1997. Flow and flexibility II: The roles of size and shape in determining wave forces on the bull kelp, *Nereocystic luetkeana*. J. Exp. Biol. **200**: 3165–3183.

Denny, M. W., P. Gaylord, B. Helmuth, and T. Daniel. 1998. The menace of momentum: Dynamic forces on flexible organisms. Limnol. Oceanogr. **43**: 955–968. doi:10.4319/lo.1998.43.5.0955

Denny, M., and B. Gaylord. 2002. The mechanics of wave-swept algae. J. Exp. Biol. **205**: 1355–1362.

Elwany, M. H. S., C. O'Reilly, R. T. Guza, and R. E. Flick. 1995. Effects of Southern California kelp beds on waves. J. Waterw. Port Coast. Ocean Eng. **121**: 143–150. doi:10.1061/(ASCE)0733-950X(1995)121:2(143)

Fonseca, M. S., S. Fisher, J. C. Zieman, and G. W. Thayer. 1982. Influence of the seagrass, Zostera marina, on

current flow. Estuar. Coast. Shelf Sci. **15**: 351–364. doi:10.1016/0272-7714(82)90046-4

Fonseca, M. S., and J. A. Cahalan. 1992. A preliminary evaluation of wave attenuation by four species of seagrass. Estuar. Coast. Shelf Sci. **35**: 565–576. doi:10.1016/S0272-7714(05)80039-3

Gaylord, B., M. W. Denny, and M. A. R. Koehl. 2003. Modulation of wave forces on kelp canopies by alongshore currents. Limnol. Oceanogr. **48**: 860–871. doi:10.4319/lo.2003.48.2.0860

Gaylord, B., M. W. Denny, and M. A. R. Koehl. 2008. Flow forces on seaweeds: Field evidence for roles of wave impingement and organism inertia. Biol. Bull. **215**: 295–308. doi:10.2307/25470713

Graham, M., C. Harrold, S. Lisin, K. Light, J. Watanabe, and M. Foster. 1997. Population dynamics of giant kelp *Macrocystis pyrifera* along a wave exposure gradient. Mar. Ecol. Prog. Ser. **148**: 269–279. doi:10.3354/meps148269

Greenberg, R., J. Maldonado, S. Droege, and M. McDonald. 2006. Tidal marshes: A global perspective on the evolution and conservation of their terrestrial vertebrates. BioScience **56**: 675–685. doi:10.1641/0006-3568(2006)56[675:TMAGPO]2.0.CO;2

Gribsholt, B., and others. 2007. Nitrogen assimilation and short term retention in a nutrient-rich tidal freshwater marsh—A whole ecosystem 15N enrichment study. Biogeosciences **4**: 11–16. doi:10.5194/bg-4-11-2007

Hepburn, C. D., D. Holborow, S. R. Wing, R. D. Frew, and C. L. Hurd. 2007. Exposure to waves enhances the growth rates and nitrogen status of the giant kelp *Macrocystis pyrifera*. Mar. Ecol. Prog. Ser. **399**: 99–108. doi:10.3354/meps339099

Hurd, C. L. 2000. Water motion, marine macroalgal physiology, and production. J. Phycol. **36**: 453–472. doi:10.1046/j.1529-8817.2000.99139.x

Hurd, C. L., J. Harrison, and L. D. Druehl. 1996. Effect of seawater velocity on inorganic nitrogen uptake by morphologically distinct forms of *Macrocystis integrifolia* from wave-sheltered and exposed sites. Mar. Biol. **126**: 205–214. doi:10.1007/BF00347445

Hurd, C. L., C. L. Stevens, B. E. Laval, G. A. Lawrence, and P. J. Harrison. 1997. Visualization of seawater flow around morphologically distinct forms of the giant kelp *Macrocystis integrifolia* from wave-sheltered and exposed sites. Limnol. Oceanogr. **42**: 156–163. doi:10.4319/lo.1997.42.1.0156

Hurd, C. L., and C. A. Pilditch. 2011. Flow-induced morphological variations affect diffusion boundary-layer thickness of *Macrocystis pyrifera* (Heterokontophyta, Laminariales). J. Phycol. **47**: 341–351. doi:10.1111/j.1529-8817.2011.00958.x

Jackson, G. A., and C. D. Winant. 1983. Effect of a kelp forest on coastal currents. Cont. Shelf Res. **2**: 75–80. doi:10.1016/0278-4343(83)90023-7

Kastler, J. A., and P. L. Wiberg. 1996. Sedimentation and boundary changes of Virginia salt marshes. Estuar. Coast. Shelf Sci. **42**: 683–700. doi:10.1006/ecss.1996.0044

Knutson, P. L., A. Brochu, W. N. Seelig, and M. Inskeep. 1982. Wave damping in *Spartina alterniflora* marshes. Wetlands **2**: 87–104. doi:10.1007/BF03160548

Koehl, M. A. R. 1984. How do benthic organisms withstand moving water? Am. Zool. **24**: 57–70. doi:10.1093/icb/24.1.57

Koehl, M. A. R., and S. A. Wainwright. 1977. Mechanical adaptations of a giant kelp. Limnol. Oceanogr. **22**: 1067–1071. doi:10.4319/lo.1977.22.6.1067

Koehl, M., and R. Alberte. 1988. Flow, flapping, and photosynthesis of *Nereocysis luetkeana*: A functional comparison of undulate and flat blade morphologies. Mar. Biol. **99**: 435–444. doi:10.1007/BF02112137

Koehl, M. A. R., W. Silk, H. Liang, and L. Mahadevan. 2008. How kelp produce blade shapes suited to different flow regimes: A new wrinkle. Integr. Comp. Biol. **48**: 834–851. doi:10.1093/icb/icn069

Luhar, M., and H. M. Nepf. 2011. Flow-induced reconfiguration of buoyant and flexible aquatic vegetation. Limnol. Oceanogr. **56**: 2003–2017. doi:10.4319/lo.2011.56.6.2003

Luhar, M., and H. M. Nepf. 2016. Wave-induced dynamics of flexible blades. J. Fluids Struct. **61**: 20–41. doi:10.1016/j.jfluidstructs.2015.11.007

Marchant, R., T. Stevens, S. Choukroun, G. Coombers, M. Santarossa, J. Whitney, and P. Ridd. 2014. A buoyant tethered sphere for marine current estimation. IEEE J. Ocean. Eng. **39**: 2–9. doi:10.1109/JOE.2012.2236151

Möller, I., T. Spencer, J. R. French, D. J. Leggett, and M. Dixon. 1999. Wave transformation over salt marshes: A field and numerical modelling study from North Norfolk, England. Estuar. Coast. Shelf Sci. **49**: 411–426. doi:10.1006/ecss.1999.0509

Mullarney, J. C., and S. M. Henderson. 2010. Wave-forced motion of submerged single-stem vegetation. J. Geophys. Res. **115**: C12061. doi:10.1029/2010JC006448

Mullarney, J. C., and S. M. Henderson. In press. The effect of marine vegetation on shorelines. *In* V. Panchang and J. Kaihatu [eds.], Advances in coastal hydraulics. World Scientific Publishing Ltd.

Nepf, H. M. 1999. Drag, turbulence and diffusion in flow through emergent vegetation. Water Resour. Res. **35**: 479–489. doi:10.1029/1998WR900069

North, W. J. 1971. The biology of giant kelp beds (*Macrocystis*) in California. Nova Hedwig. Beih. **32**: 1–600.

Reed, D. C., and M. S. Foster. 1984. The effects of canopy shadings on algal recruitment and growth in a giant kelp forest. Ecology **65**: 937–948. doi:10.2307/1938066

Reed, D. C., A. Rassweiler, and K. K. Arkema. 2008. Biomass rather than growth rate determines variation in net primary production by giant kelp. Ecology **89**: 2493–2505. doi:10.1890/07-1106.1

Riffe, K. C., S. M. Henderson, and J. C. Mullarney. 2011. Wave dissipation by flexible vegetation. Geophys. Res. Lett. **38**: L18607. doi:10.1029/2011GL048773

Rominger, J. T., and H. M. Nepf. 2014. Effects of blade flexural rigidity on drag force and mass transfer rates in model blades. Limnol. Oceanogr. **59**: 2028–2041. doi:10.4319/lo.2014.59.6.2028

Rosman, J. H., R. Koseff, S. G. Monismith, and J. Grover. 2007. A field investigation into the effects of a kelp forest (*Macrocystis pyrifera*) on coastal hydrodynamics and transport. J. Geophys. Res. **112**: C02016. doi:10.1029/2005JC003430

Rosman, J. H., W. Denny, R. B. Zeller, S. G. Monismith, and J. R. Koseff. 2013. Interaction of waves and currents with kelp forests (*Macrocystis pyrifera*): Insights from a dynamically scaled laboratory model. Limnol. Oceanogr. **58**: 790–802. doi:10.4319/lo.2013.58.3.0790

Simpson, J. H. 1969. Observations of the directional characteristics of sea waves. Geophys. J. R. Astron. Soc. **17**: 93–120. doi:10.1111/j.1365-246X.1969.tb06380.x

Stephens, T. A., and C. D. Hepburn. 2016. A kelp with integrity: Macrocystis pyrifera prioritises tissue maintenance in response to nitrogen fertilization. Oecologia **182**: 71–84. doi:10.1007/s00442-016-3641-2

Stevens, C. L., C. L. Hurd, and M. J. Smith. 2001. Water motion relative to subtidal kelp fronds. Limnol. Oceanogr. **46**: 668–678. doi:10.4319/lo.2001.46.3.0668

Stevens, C. L., C. L. Hurd, and M. J. Smith. 2002. Field measurement of the dynamics of the bull kelp *Durvillaea Antarctica* (Chamisso) Heriot. J. Exp. Mar. Biol. Ecol. **269**: 147–171. doi:10.1016/S0022-0981(02)00007-2

Stewart, H. L. 2006. Hydrodynamic consequences of flexural stiffness and buoyancy for seaweeds: A study using physical models. J. Exp. Biol. **209**: 2170–2181. doi:10.1242/jeb.02254

Thomsen, M. S., T. Wernberg, and G. A. Kendrick. 2004. The effect of thallus size, life stage, aggregation, wave exposure and substratum conditions on the forces required to break or dislodge the small kelp *Ecklonia radiata*. Bot. Mar. **47**: 454–460. doi:10.1515/BOT.2004.068

Ward, L., W. Kemp, and W. Boyton. 1984. The influence of waves and seagrass communities on suspended particulates in an estuarine embayment. Mar. Geol. **59**: 85–103. doi:10.1016/0025-3227(84)90089-6

Zedler, L., J. Callaway, and G. Sullivan. 2001. Declining biodiversity: Why species matter and how their functions might be restored in Californian tidal marshes. BioScience **51**: 1005–1017. doi:10.1641/0006-3568(2001)051[1005:DBWSMA]2.0.CO;2

Acknowledgments

We thank the PADI foundation, the University of Waikato Research Trust, and the University of Waikato Strategic Investment Fund for funding, Steve Henderson for useful discussions, Dudley Bell for invaluable assistance with diving and fieldwork and Warrick Powrie and for assistance with fieldwork during pilot experiments. We thank the two anonymous reviewers whose comments helped to substantially improve the manuscript.

Conflict of Interest

None declared.

Submitted 20 May 2016
Revised 07 February 2017
Accepted 05 April 2017

Associate editor: Josef Ackerman